

February 01, 1992

Quantum nucleation and thermal-activation of vortex rings in high-T_c superconductors

H. Jiang

A. Widom
Northeastern University

Y. Huang

T. Yuan

C. Vittoria
Northeastern University

See next page for additional authors

Recommended Citation

Jiang, H.; Widom, A.; Huang, Y.; Yuan, T.; Vittoria, C.; Chrisey, D. B.; and Horwitz, J. S., "Quantum nucleation and thermal-activation of vortex rings in high-T_c superconductors" (1992). *Electrical and Computer Engineering Faculty Publications*. Paper 111.
<http://hdl.handle.net/2047/d20002282>

Author(s)

H. Jiang, A. Widom, Y. Huang, T. Yuan, C. Vittoria, D. B. Chrisey, and J. S. Horwitz

Quantum nucleation and thermal activation of vortex rings in high- T_c superconductors

H. Jiang, A. Widom, Y. Huang, and T. Yuan

Department of Physics, Northeastern University, Boston, Massachusetts 02115

C. Vittoria

Department of Electrical Engineering, Northeastern University, Boston, Massachusetts 02115

D. B. Chrisey and J. S. Horwitz

Naval Research Laboratory, Washington, D.C. 20375

(Received 10 May 1991)

Vortex-ring nucleation by thermal activation and quantum-tunneling processes in high- T_c superconductors is discussed. The nonlinear resistance scales as $e^{-(J_v/J)^\nu}$. Thermal activation yields a critical index of $\nu=1$, while quantum tunneling (without normal current dissipation) yields a critical index of $\nu=2$. Current-voltage characteristics were measured on both disordered (low- J_c), ordered (c axis normal to the film plane, high- J_c) Y-Ba-Cu-O films, and microbridges below T_c . The data were examined in terms of both thermal-activation and quantum-nucleation models. For the disordered films, the $\nu=1$ scaling law is in reasonable agreement with data, while $\nu=2$ scaling is required to explain the results of the ordered films at low temperatures. For the microbridges, the $\nu=2$ scaling extends even to high temperatures.

I. INTRODUCTION

Vortex dynamics is of interest from a fundamental as well as an applied point of view. There are several models which have discussed the vortex dynamics, and have been referred to in the literature as the flux creep,¹⁻⁴ collective flux creep,^{5,6} flux glass,^{7,8} and two-dimensional vortex fluctuations⁹ models. The basic issue at hand is whether or not thermal energy is the only means by which vortices are activated or set in motion. It is well known that vortex motion implies an induced electric field and thereby resistance in otherwise superconducting materials. The threshold currents at which vortices induce voltages represents a limitation on potential applications of high- T_c materials.

In this paper, we discuss another mechanism for vortex dynamics applicable to type-II superconductors. Specifically, we demonstrate both theoretically and experimentally that vortex motion can also be induced quantum mechanically for temperatures well below T_c . This is true for both superconducting films and extremely narrow bridge constrictions. The flux flow resistivity, ρ , based on thermal activation of the vortex-ring motion is theoretically given by

$$\rho \sim \exp(-J_1/J). \quad (1)$$

Experimentally, we find (at low temperatures) ρ obeys the following exponential power law:

$$\rho \sim \exp[-(J_2/J)^2]. \quad (2)$$

We have postulated a quantum-tunneling model in which the radius of a vortex ring changes from relatively small value (near the coherence length ξ) to R_0 , where R_0

is the threshold radius beyond which vortex rings are free to expand and induce a voltage drop. The vortex-ring quantum-nucleation transition probability is governed by a tunneling probability through an energy barrier. The resultant resistivity from this model obeys Eq. (2).

In Sec. II, we formulate the model on the basis of a phenomenological free energy. The free energy consists of the vortex-ring self-energy, and the interaction energy of vortex ring and the driving current equivalent to the Lorentz force. The free energy is a maximum at $R_n = c\tau/\Phi_0 J$, where τ is the "tension" of the vortex ring viewed as a closed string. Hence, the transition is defined between values of R below R_n , say ($R \sim \xi$) and R greater than R_n , i.e., ($R_0 = 2c\tau/\Phi_0 J$). The WKB method (without normal current dissipation) is used to calculate the transition probability. In Sec. III, the sample preparation and experimental details are described. In Sec. IV the data are presented in which the tunneling model is fitted to the film data at low temperatures and microbridge data over a wide temperature range. Data characterized by low- J_c films is in good agreement with the exponential linear power law. However, the deduced values of J_1 and J_2 from these models are much higher than the measured J_c values. This discrepancy will be addressed theoretically in the future, where quantum tunneling with dissipation is included in the theory. Finally, conclusions are discussed in Sec. V.

II. THEORY

In the Ginzburg-Landau model of type-II superconductors, the vortex line can be viewed as a string with tension (energy per unit length) τ , given by

$$\tau = \left[\frac{\Phi_0}{4\pi\lambda} \right]^2 \ln \kappa, \quad (3)$$

where $\kappa = \lambda/\xi$, λ is the London penetration depth, ξ is the vortex core coherence length (or equivalently the size of superconducting pair), and the magnetic flux quantum is $\Phi_0 = hc/q$ with $q = 2e$. On the other hand, the vortex line should also be viewed as a string with *mass per unit length*,¹⁰

$$\mu = \left[\frac{\Phi_0}{4\pi c \xi} \right]^2. \quad (4)$$

If a current density is flowing in a superconducting film (and the film is not extremely thin), then it is possible that vortex rings will be nucleated in the plane normal to the direction of current flow, see Fig. 1. The free energy of the vortex ring in the presence of an applied current is

$$U(R) = 2\pi R \tau - \frac{\Phi_0}{c} J \pi R^2, \quad (5)$$

where R is the radius of the vortex ring, J is the current density flow through the superconductor. The first term in Eq. (5) is the self-energy of a vortex ring, while the second term is the interaction energy of vortex ring and applied current which plays a role equivalent to the Lorentz force. A sketch of $U(R)$ is shown in Fig. 2.

A nucleation radius R_n exists for the ring such that rings of radius $R < R_n$ have not the classical energy to grow ever larger, and rings with radius $R > R_n$ find it classically favorable (with respect to energy) to grow ever larger giving rise to the electric fields. The nucleation radius of ring is given at the maximum of energy in Eq. (5),

$$R_n = \frac{c\tau}{\Phi_0 J} = \frac{c\Phi_0}{16\pi^2 \lambda^2 J} \ln \kappa. \quad (6)$$

The nucleation radius cannot be less than the size of vortex core (i.e., the thickness of the vortex ring). By demanding that R_n/ξ be at least unity in Eq. (6), we get an absolute maximum current density flow in the superconducting film. This turns out to be close to what others have called the *depairing current*,

$$J_d = \frac{c\Phi_0 \kappa}{16\pi^2 \lambda^3} \ln \kappa. \quad (7)$$

The nucleation energy, therefore, is

$$U_n = U(R_n) = \tau \pi R_n = \frac{\Phi_0^2}{16\pi\lambda} \frac{\ln \kappa}{\kappa} \frac{J_d}{J}. \quad (8)$$

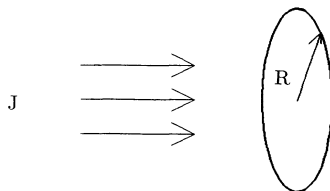


FIG. 1. Diagram of vortex-ring nucleation.

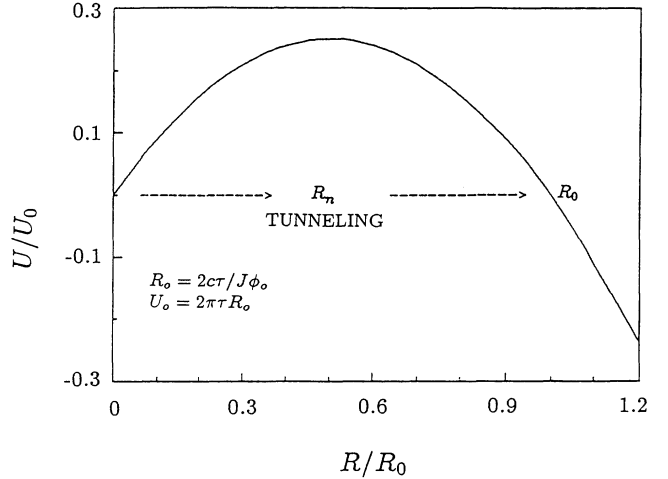


FIG. 2. Vortex-ring free energy as a function of vortex-ring radius in normalized units.

The mass of the ring at nucleation radius is given by

$$M_n = 2\pi R_n \mu = \frac{\Phi_0^2}{8\pi c^2 \xi} \frac{J_d}{J}. \quad (9)$$

From a classical point of view, only vortex rings with radius larger than R_n will be energetically free to expand or break up into vortex lines. The vortex ring can escape from being pinned by thermal activation over the energy barrier given in Eq. (5). The thermal nucleation rate is dominated by the activation factor

$$\Gamma = e^{-U_n/k_B T}. \quad (10)$$

If we denote the critical escape current density as

$$J_1 = \frac{\Phi_0^2}{16\pi\lambda} \frac{\ln \kappa}{\kappa} \frac{J_d}{k_B T}, \quad (11)$$

then we have

$$\Gamma = e^{-J_1/J}. \quad (12)$$

From a quantum-mechanics point of view, the radius of vortex ring can change from a very small value, say (ξ), to R_0 by the quantum-tunneling process. The transition probability may be calculated by using the WKB approximation¹¹ to reasonable accuracy (but without normal current dissipation)

$$P_0 = \exp(-U_n/\hbar\Omega_0), \quad (13)$$

where

$$\Omega_0 = \sqrt{U''(R)/M_n} = \frac{c}{\lambda} \sqrt{\ln \kappa} \frac{J}{J_d}. \quad (14)$$

This yields

$$P_0 = e^{-(J_2/J)^2}, \quad (15)$$

where

$$J_2 = \frac{\Phi_0^2}{16\pi\kappa\hbar c} \sqrt{\ln \kappa} J_d. \quad (16)$$

High- T_c superconductors are anisotropic. The London penetration depth depends on whether the screening currents move in the ab planes (λ_{\parallel}) or whether the screening currents are normal to the planes (λ_{\perp}). The anisotropy parameter $\alpha = (\lambda_{\perp}/\lambda_{\parallel})$ is about a factor of 3 for the samples here of interest. However, the coherence length anisotropy ratio $\alpha = (\xi_{\parallel}/\xi_{\perp})$ is inversely proportional to the London penetration depth ratio so that $\lambda_{\perp}\xi_{\perp} = \lambda_{\parallel}\xi_{\parallel}$. Thus, the quantum-tunneling current J_2 does not depend very strongly on anisotropy effects apart from the $\ln\kappa$ factor which increases by 20%. On the other hand, the thermal activation current J_1 depends much more strongly on anisotropy effects, decreasing by a factor of $\sim\alpha^2$, i.e., 10, since, in this case, the coherence length enters weakly into the problem.

The nucleated vortex ring (by either thermal-activation or quantum-tunneling processes) produces electric fields as a current is driven through the superconductor. The resulting voltage is proportional to the probability of free vortex-ring production. The signature for such effects is a nonlinear current-voltage characteristic

$$E = \rho J e^{-(J_v/J)^{\nu}}, \quad (17)$$

where ρ is the normal flux-flow resistivity. When $\nu=1$, Eq. (17) represents the thermal-activation process while $\nu=2$ represents the quantum tunneling of free vortex-ring nucleation.

III. SAMPLE PREPARATION

Several $\text{YBa}_2\text{Cu}_3\text{O}_{7-x}$ films prepared by either laser ablation or ion beam sputtering were used in our experiment. High-quality Y-Ba-Cu-O thin films were prepared (using the pulsed laser deposition techniques) with a thickness of ≈ 5000 Å. Films were deposited on polished $\text{MgO}(100)$ substrates at 750°C , and then quenched *in situ*. X-ray-diffraction measurements indicated the samples were c -axis oriented perpendicular to the film plane. Pole figure analysis of the (0,1,2) peak indicated some misorientation in the a - b plane peaked strongly at 90° and to a much lesser extent at 45° . The thin films studied had room-temperature resistivity about $300 \mu\Omega\text{cm}$, and showed sharp superconducting transitions ($\Delta T_c \sim 0.5$ K) at $T_c \approx 92$ K. The critical current densities at 77 K were typically from $2\sim 4 \times 10^6$ A/cm². Disordered low- J_c films were made by ion beam sputtering on $\text{YSZ}(100)$ substrates, where YSZ is yttria-stabilized cubic zirconia. The target was first heated to 950°C , and then slowly cooled at a rate of 60°C/h . The sputtering rate was ~ 2.8 Å/sec. All as-deposited films were insulators before post-annealing. The films were thermally annealed in a furnace tube at an oxygen flow rate of 1.2 l/min. The annealing temperature was increased linearly (360°C/h) from room temperature to 700°C , held at that temperature for ~ 40 min, then increased to 870°C in 1 h, held at 870°C for 1 h, and then slowly cooled to room temperature in 15 h. For comparison purposes, we chose a sputtering film with very low J_c ($10^3\sim 10^4$ A/cm²) and broad transition temperature. Typical R - T curves of high- and low- J_c films are shown in Fig. 3.

The Y-Ba-Cu-O strips were fabricated with widths of

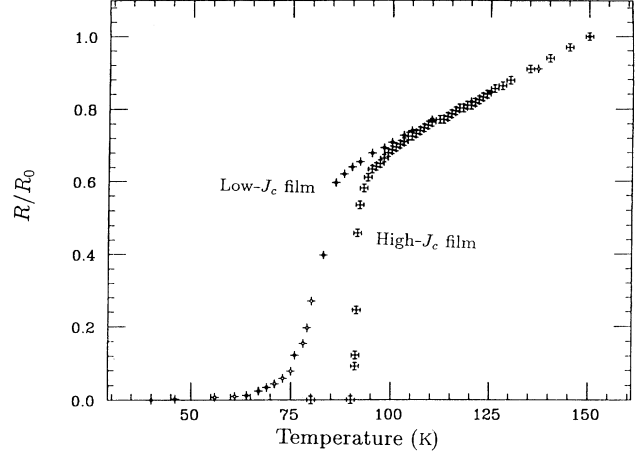


FIG. 3. Typical resistance as a function of temperature for low- J_c and high- J_c films.

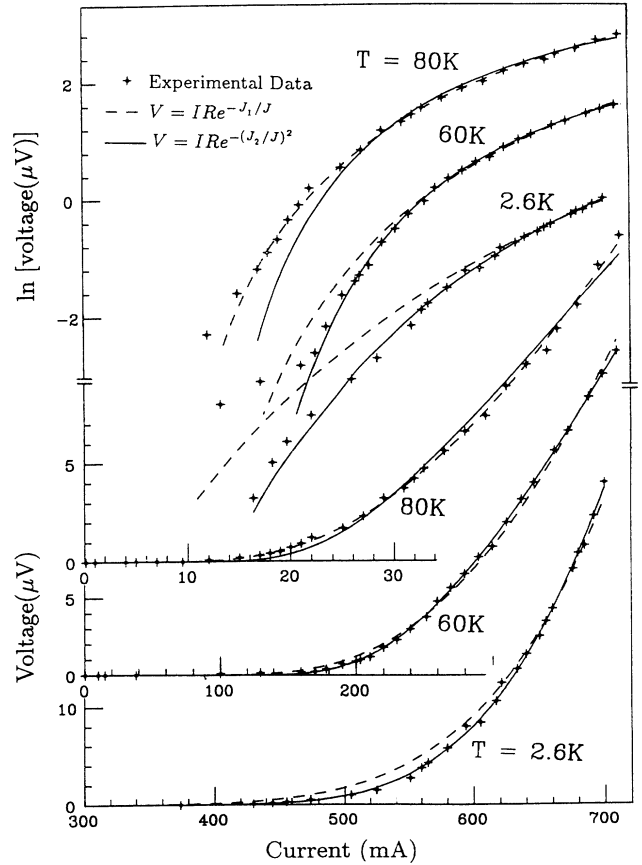


FIG. 4. I - V and I - $\ln V$ curves of high- J_c films at temperatures of 2.6, 60, and 80 K. The stars are experimental data, dashed lines are fitting curves with $\nu=1$ scaling, and solid lines are fitting curves with $\nu=2$ scaling. The logarithmic scales for 60 and 2.6 K are not shown.

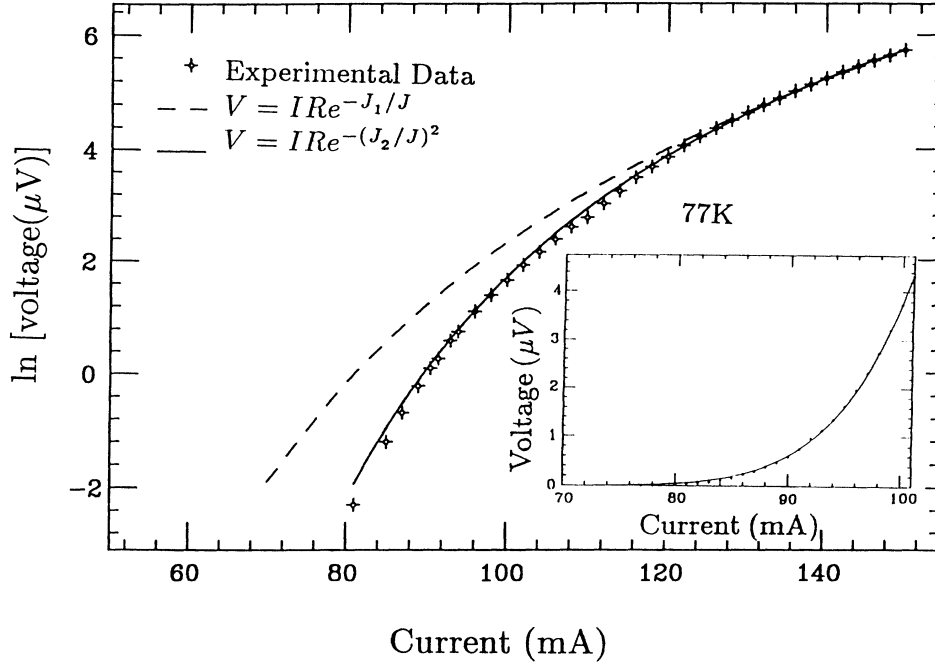


FIG. 5. Current-voltage characteristics of a microbridge at 77 K plotted in a I - $\ln V$ scale. The inset is a I - V curve obtained near J_c .

500 Å to 1 mm by photolithography, chemical etching, and ion-beam direct milling, a detailed procedure was given in Ref. 12.

Standard four-point probe dc measurements were performed on these strips. To obtain high-quality leads onto the films, the films were first cleaned with methanol, and then a layer of silver bar was evaporated onto the contact area. Indium soldering was employed to connect silver wires to the silver bar. Typical contact resistivity was $\sim 10^{-5} \Omega \text{ cm}^2$ at room temperature. A Keithly programmable current source was used. A Keithly 182 nanovoltmeter was employed for voltage measurements, with a resolution of $\sim 10^{-9} \text{ V}$. An Oxford CF-1204 continuous liquid-He flow cryostat was used to cool the samples, the temperature range was 2.6–300 K. An Oxford ITC4 temperature controller with a Rh-Fe thermal sensor was employed to control the temperature with an error $\leq 0.1 \text{ K}$.

IV. RESULTS AND DISCUSSION

In Fig. 4, current-voltage characteristics were plotted in both V - I and $\ln V$ - I scales for a high- J_c film ($3 \times 10^6 \text{ A/cm}^2$ at 77 K) at temperatures of 2.6, 60, and 80 K, respectively. The stars are experimental data, the dashed lines are fitting curves with $\nu=1$, and the solid line are fitting curves with $\nu=2$. The logarithmic scale is only for curves obtained at 80 K, the scales for 60 and 2.6 K are not shown. At low temperatures, say 2.6 K, the fit to the experimental data is vastly improved if $\nu=2$ instead of $\nu=1$. In the fitting process, we also used the combination of two models ($Ae^{-J_1/J} + Be^{-(J_2/J)^2}$) to fit the data. The confidence level was highest when $A \sim 0$ and $B \sim 1$ at low

temperatures. At 80 K, the $\nu=1$ scaling is in better agreement with experimental data. A physical interpretation of our data is that, at low temperatures, the thermal vibration of vortex ring is small. Quantum tunneling becomes the major process. When the temperature is near T_c , the thermal energy of vortex rings increases sufficiently to overcome the energy barrier.

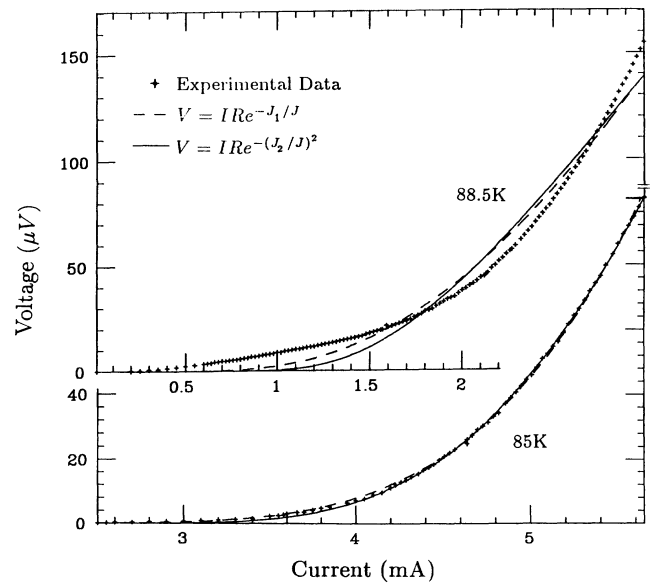


FIG. 6. The I - V data and fitting curves of a microbridge at 85 and 88.5 K.

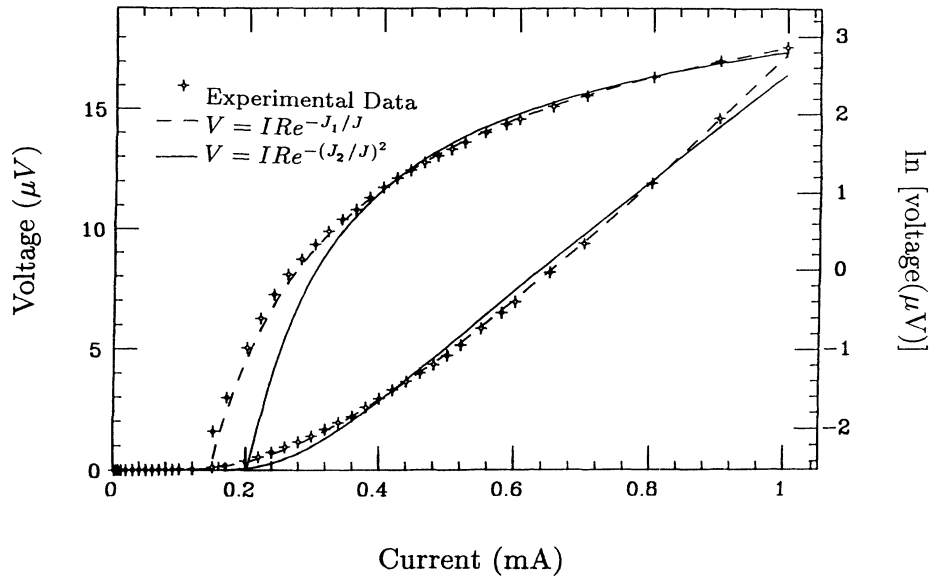


FIG. 7. Low- J_c film I - V characteristics at 3 K. The reader is referred to the scale on the right-hand side of the figure for logarithmic scale.

Therefore, the thermal-activation process appears to be dominant at high temperatures.

The I - V characteristics were measured on a microbridge with width of 500 Å. The critical current density of this bridge¹² was 3.6×10^8 A/cm² at 77 K. Experimental data and fitting curves are shown in Figs. 5 and 6. The dashed line corresponds to $\nu=1$ scaling, while the solid line with $\nu=2$. In Fig. 5, the $\ln V$ versus current at 77 K are shown with fitting curves. The inset in Fig. 5 is the I - V curve obtained near J_c and the experimental points fit the $\nu=2$ scaling quite well. Clearly, at 77 K the quantum nucleation of vortex rings is still playing a major role in microbridges. This is not very surprising to us. First of all, the J_c of the microbridge is extremely high (more than 2 orders higher than that of films). This implies a very small vortex ring ($R \leq 100$ Å). The size of the ring is in the same order of the bridge width; therefore, the edge pinning is very important. If we consider the contribution of edge pinning, the effective energy barrier will be very high and narrow, where the vortex ring requires additional energy beyond Eq. (5) to overcome the barrier by thermal activation. Quantum tunneling through the barrier allows for vortices to move. At 85 K, both models approximately fit the experimental data but the agreement of fit is poor at $T=88.5$ K, see plots in Fig. 6. The models considered here are not valid near T_c since fluctuations near the critical temperature have not been taken into account.

For sputtering films characterized by low J_c ($J_c = 5 \times 10^3$ A/cm² at 77 K), the $\nu=1$ scaling agrees with experiment data at most temperatures. The results are shown in Fig. 7. For the low- J_c film, the vortex-ring model is inappropriate. We can estimate the radius of

the ring by using Eq. (6) to be in the order of a few thousand microns, which is much bigger than the thickness of the film (5000 Å). Hence, this can be viewed as a vortex-antivortex pair excitation. At low temperatures, films characterized by low J_c also exhibit $\nu=1$ scaling. The tunneling model can be made to fit a $\nu=1$ scaling law for vortex-antivortex nucleation¹³ (instead of vortex rings) where the thermal-activation model predicts scaling. Hence, at low temperatures and for low- J_c films, it is *inconclusive* to choose one model over the other. For films characterized by high J_c , the data only fit a $\nu=2$ scaling at low temperatures, which our tunneling model does predict.

V. CONCLUSION

We have demonstrated that the vortex dynamics could be either thermally activated or quantum-mechanically induced. In high- J_c superconducting films, the quantum nucleation of vortex rings plays a major role when the temperature is substantially below T_c . In high- J_c microbridges, quantum tunneling of vortex rings occurs even at high temperatures (about 10 K below T_c). For low- J_c superconducting films, the quantum-tunneling or thermal-activation models may both be involved to explain our experimental results at low temperatures. The discrepancy between deduced J_1 and J_2 and J_c may be due to the neglect of the inclusion of dissipation in the tunneling barrier factor, which would tend to increase the tunneling rates.

ACKNOWLEDGMENT

We wish to thank the NSF for support.

- ¹P. W. Anderson and Y. B. Kim, Rev. Mod. Phys. **36**, 39 (1964).
²M. R. Beasley, R. Labusch, and W. W. Webb, Phys. Rev. **181**, 682 (1969).
³T. T. M. Palstra, B. Batlogg, R. B. Van Dover, L. F. Schneemeyer, and J. V. Waszczak, Appl. Phys. Lett. **54**, 763 (1989).
⁴S. Martin, A. T. Fiory, R. M. Fleming, G. P. Espinosa, and A. S. Cooper, Phys. Rev. Lett. **62**, 677 (1989).
⁵P. G. De Gennes and J. Mantricon, Rev. Mod. Phys. **36**, 45 (1964).
⁶M. V. Feigel'man, V. B. Geshkenbein, A. I. Larkin, and V. M. Vinokur, Phys. Rev. Lett. **63**, 2303 (1989).
⁷M. P. A. Fisher, Phys. Rev. Lett. **62**, 1415 (1989).
⁸R. H. Koch, V. Fogliette, V. J. Gallagher, G. Koren, A. Gupta, and M. P. A. Fisher, Phys. Rev. Lett. **63**, 1511 (1989).
⁹H. J. Jensen and P. Minnhagen, Phys. Rev. Lett. **66**, 1630 (1991).
¹⁰A. Widom, R. Karim, H. How, and C. Vittoria, in *Macroscopic Quantum Phenomena*, edited by T. D. Clark *et al.* (World Scientific, Singapore, 1991).
¹¹A. Widom and T. D. Clark, Phys. Rev. Lett. **48**, 63 (1982).
¹²H. Jiang, Y. Huang, H. How, S. Zhang, C. Vittoria, A. Widom, D. B. Chrisey, J. S. Horwitz, and R. Lee, Phys. Rev. Lett. **66**, 1785 (1991).
¹³J. H. Miller (unpublished), and (private communication).